A vortex isolation and removal algorithm for numerical weather prediction model tropical cyclone applications

JAMES

JOURNAL OF ADVANCES IN MODELING EARTH SYSTEMS

Henry R. Winterbottom[1] and Eric P. Chassignet[2]

[1] Cooperative Institute for Research in Environmental Sciences, Earth System Research Laboratory, NOAA, 325 Broadway, Boulder, CO 80303, USA.
[2] Center for Ocean-Atmospheric Prediction Studies, Florida State University, Tallahassee, FL 32306, USA.

Inserting an externally defined (i.e., synthetic) tropical cyclone (TC) vortex into numerical weather prediction (NWP) model analyses requires that an existing TC vortex first be removed. Similarly, statistical-dynamical forecasting methods require that the larger-scale environmental attributes of the flow be separated (and preserved) from those on the smaller meso- and TC vortex scales. The existing operational methods to accomplish such tasks are optimized particularly for the respective models grid spacing resolution and thus are not general when applied to finer resolution analyses. Further, the existing methods often adhere to rigid assumptions regarding the size and structure of the TC. A methodology is provided in this study to overcome these limitations. This is accomplished through analyzing the features of the NWP model analysis (e.g., the variables in the vicinity of the TC) and then systematically removing the TC through the application of both a smoothing operator and a subsequent statistical evaluation of the smoothed analysis variable. The value of our methodology is determined when analyzing the results from experiments initialized from an analysis containing TCs and those initialized from analyses without the respective TCs. This methodology is also robust for it does not require a tuning of parameters relative to varying grid-spacing resolutions and may thus benefit the statistical-dynamical TC intensity prediction schemes.

1. Introduction

The large-scale (synoptic) environment surrounding a tropical cyclone (TC) has been identified as a primary mechanism governing the future track [*Fiorino and Elsberry*, 1989; *Mathur*, 1991; *Goerss*, 2006; *Ritchie and Frank*, 2007] and the future intensity of a TC [*DeMaria et al.*, 1994, 2005; *Knaff et al.*, 2005; *Sampson et al.*, 2008; *DeMaria*, 2010]. The dynamical importance for preserving the synoptic environment was illustrated by *Kurihara et al.* [1995] when forecasting the track and intensity for TC Florence (1988). *DeMaria et al.* [1994, 2005], and more recently *DeMaria* [2010] provided an assessment of the predictability improvements when preserving the synoptic environment using statistical intensity prediction schemes such as the Statistical Hurricane Intensity Prediction Scheme (SHIPS) and the Logistic Growth Equation Model (LGEM). Therefore, an accurate evaluation of the environment surrounding the TC is warranted if both dynamical and statistical based TC predictions are to improve.

There have been several different methods proposed to separate the TC from the larger, synoptic-scale environmental flow. Each of these methods have been developed and tuned relative to the experiment and, as a result, utilize various degrees of complexity for the diagnostics required to separate those components of the atmosphere which are related to the TC and those which are related to the environment. *Velden and Leslie* [1991], while evaluating the environmental steering levels acting to advect the TCs within the Australian region, utilized a simple method to separate the TC from the environmental flow. *Velden and Leslie* [1991] assume that the TC is axisymmetric and remove it by first setting all values within the operationally analyzed TC outer-most closed isobar to zero and then performing a bi-linear interpolation (using each of the points just beyond the specified radius) as a proxy for the environmental flow where the TC once existed. Alternative approaches have applied low-pass spatial filters to diagnose the environmental features impacting the TC

To whom correspondence should be addressed.
H. R. Winterbottom, Cooperative Institute for Research in Environmental Sciences, Earth System Research Laboratory, NOAA, 325 Broadway, Boulder, CO 80303, USA.
henry.winterbottom@noaa.gov

motion [i.e., *DeMaria*, 1985; *Elsberry et al.,* 1993] and for the relocation of a TC within model analyses [*Lord*, 1991; *Hsiao et al.*, 2010]. Additional methodologies, including potential vorticity (PV) analysis and inversion have also been explored (B. H.-A. Tang, personal communication, 2010).

The current operational method to remove a TC circulation was developed at the National Oceanic and Atmospheric Administration (NOAA) Geophysical Fluid Dynamics Laboratory (GFDL) [*Kurihara et al.*, 1993, 1995]. This methodology, prior to removing the TC vortex, partitions the respective analysis variable into a *basic* and a *disturbance* component. The disturbance component is further partitioned to include an *analyzed* vortex component which contains the anomalies related to the presence of the TC vortex. The size for the analyzed TC vortex is case dependent and estimated as described by *Kurihara et al.* [1995]. The TC vortex is separated from the flow using multiple iterations of a 3-point smoothing operator and a spatial filter. The strength of the filter is controlled using coefficients determined empirically for the $1° \times 1°$ model analysis providing the input for the GFDL TC prediction model. Finally, the *environmental* component is the sum of the basic state and the disturbance state without the analyzed TC vortex [see *Kurihara et al.*, 1993, equation 3.2].

Applying the GFDL methodology to model state variables defined on grids that are of higher horizontal grid-spacing resolution may fail to entirely remove the TC vortex related anomalies and as a result can introduce artificial gradients when the environmental component for the respective analysis variable is reconstructed. These shortcomings may be overcome by varying both the number of spatial filter iterations and the strength of the spatial filter. However, these modifications require both experimentation and tuning for the GFDL algorithm as both the analysis and (more importantly) the grid-spacing resolutions vary. In this study, a TC vortex removal algorithm is proposed which (1) does not require tuning as a function grid-spacing resolution, (2) does not make stringent assumptions regarding the structure of the TC vortex, and (3) diagnoses the thermodynamic and kinematic aspects of the TC related flows separately. The algorithm is designed within the framework of the Advanced Weather Research and Forecasting (WRF-ARW) [*Skamarock et al.*, 2005] model but is applicable to most numerical weather prediction (NWP) models. The remainder of this manuscript is organized as follows: section 2 provides the TC isolation and removal algorithm while section 3 examines a WRF-ARW forecast using the analysis fields from which all TCs have been removed. Finally, section 4 provides a conclusion from this study while presenting some applications of the algorithm.

2. Tropical Cyclone Isolation and Removal Algorithm

This section provides a methodology to first locate and then subsequently remove TC vortices within NWP model analyses. Although it is impossible to *completely* remove the TC, due primarily to the TC's modulation of the atmosphere at a broad spectrum of scales, our goal is to estimate both the kinematic and thermodynamic NWP model analysis variables as though the TC were not present.

2.1. Determining the TC Vortex Kinematic and Thermodynamic Analysis Variable Removal Regions

Prior to applying the TC removal algorithm, the position for the respective TC vortex (within the NWP model analysis) must be determined. The importance of this step becomes clear when the TC vortex within the NWP model analysis is grossly displaced from the *observation* position. The implications and consequences resulting from different locations for a respective analysis and observed TC is discussed by *Mathur* [1991] and *Kurihara et al.* [1993]. The location of the NWP model analysis TC vortex and the subsequent specification of the TC vortex removal region is accomplished in several steps. The first-step estimates the position for the analysis TC vortex using the methodology discussed by *Marchok* [2002]. Once the position is determined, the next step is to estimate the *geometric center* (or centroid) position of the respective TC vortex at each NWP model analysis level. The centroid positions are estimated from the methodology provided by *Kurihara et al.* [1995]. This second-step is an important consideration when applying the algorithm to a TC vortex that is tilted (with height) as a result of an environment with appreciable wind shear and is a unique feature of the methodology provided in this study for it enables the respective kinematic and thermodynamic regions to both telescope and stagger as a function of analysis level.

We next define separate kinematic and thermodynamic analysis variable removal regions that are relative to the centroid position at each analysis level. The radial size for the (possibly) polygonal kinematic variable regions is estimated using the centroid-relative tangential wind criteria discussed by *Kurihara et al.* [1995]. Observational studies providing composites for both the kinematic and thermodynamic structures of TCs [*LaSeur and Hawkins*, 1963; *Shea and Gray*, 1973; *Gray and Shea*, 1973; *Hasler and Morris*, 1986; *Marks and Houze*, 1987; *Franklin et al.*, 1988, 1993] suggest that the TC's thermodynamic influence is often larger than the respective kinematic influence. Therefore, the thermodynamic variable removal regions are defined by a circle, centered at the respective analysis level centroid position, which is scaled relative to the maximum radial size for the corresponding kinematic variable region. For the purposes of this study, a scaling factor of 1.25 was found to be sufficient.

The final step involves refining the depth for the kinematic and thermodynamic model removal regions to the depth of the troposphere. This depth is estimated on a case-by-case basis using the elevation of *dynamic* tropopause. The potential vorticity (PV) is computed using Ertel's formulation

Table 1. Empirically Determined Analysis Variable Convergence Values ($\Delta\sigma^2$) for the TC Vortex Removal Algorithm.

Model State Variable (units)	*u* (m/s)	*v* (m/s)	*T* Anomaly (K)	φ Anomaly (m)	*RH* Anomaly (%)	P_{slp} (Pa)
$\Delta\sigma^2$	1.0×10^{-4}	1.0×10^{-4}	1.0×10^{-5}	1.0×10^{-3}	1.0×10^{-4}	1.0×10^{-4}

(described by *Gill* [1982]) and a *top-down* search for the respective PV isosurface. For this study, the 2-PVU isosurface (i.e., dynamic tropopause) between 150 hPa and 450 hPa is located using cubic-spline interpolation. Similar to the threshold radial distance values constraining the radial extent for the kinematic filter [*Kurihara et al.*, 1995], the 150-hPa and 450-hPa isobars provide upper- and lower limits respectively for the height of the dynamic tropopause.

2.2. Removal of the Model Analysis TC Vortex

As stated previously, we seek to estimate the analysis variables in the absence of the TC vortex. The anomalous features, for the respective model state variables, are removed using the following 9-point (spatial) smoothing operator:

$$H^o_{L,K} = \frac{1}{9} \sum_{k=K-1}^{k=K+1} \sum_{l=L-1}^{l=L+1} H^i_{l,k}$$

Here, (L,K) denotes the respective (x,y) grid coordinate for which the *smoothed* model state variable (H^o) is

computed from 9-neighboring *unsmoothed* model state variables (H^i). Following the application of the smoothing operator, the change in spatial variance is evaluated as

$$\Delta\sigma^2 = \left| \sigma_t^2 - \sigma_{t-1}^2 \right|$$

where σ_t^2 is the *current* spatial variance and σ_{t-1}^2 is the spatial variance computed from the previous application of the smoothing operator. The application of the smoothing operator and the subsequent evaluation of the change in spatial variance continues until $\Delta\sigma^2$ approaches a specified (empirically defined) value. The threshold $\Delta\sigma^2$ values for the respective analysis variables, examined in this study, are provided in Table 1. Figure 1 illustrates the National Centers for Environmental Prediction (NCEP) Global Forecasting System (GFS) sea-level pressure (Pa; contour) and lowest-model level wind (kts; colored vectors) analyses before (a) and after (b) the application of the TC vortex removal algorithm to the 0000 UTC 01 September analysis for TC Gustav (2008). The solid and dashed red lines indicate the kinematic and thermodynamic model analysis variable removal regions respectively. The most notable feature,
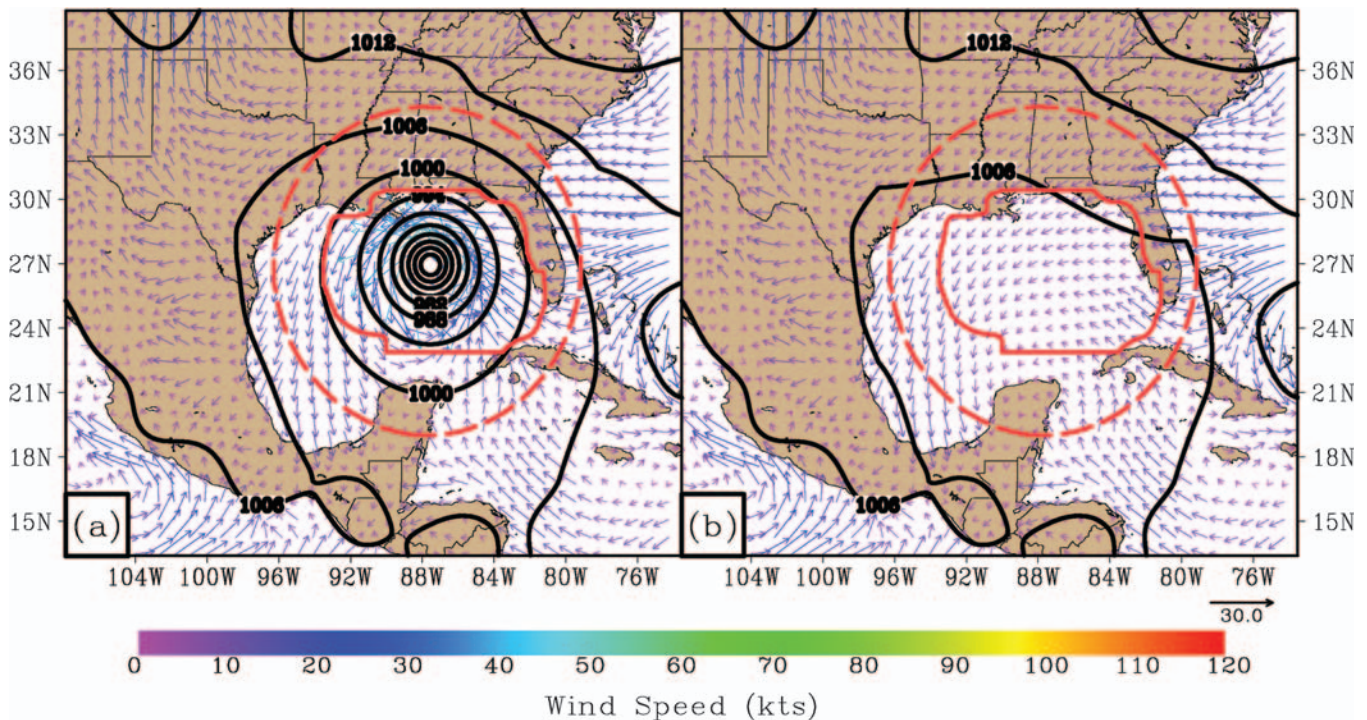

Figure 1. The lowest model level (e.g., near surface) wind speed magnitude (kts; colored vectors) and the sea-level pressure (Pa; contour) (a) before and (b) after the application of the TC vortex removal algorithm to the 0000 UTC 01 September GFS analysis for TC Gustav (2008) interpolated to a 6.0-km WRF-ARW model simulation grid. The solid and dashed red lines indicate the kinematic and thermodynamic filter regions respectively.

when comparing Figures 1a and 1b is that the winds and sea-level pressure values due to the TC vortex have been removed while simultaneously maintaining continuity of the flow as illustrated by the orientation of the wind vectors along the boundaries of the TC vortex removal region. Figure 2 provides a cross-section both before (a) and after (b) the removal procedure is applied to the same NCEP GFS analysis. Here, the wind speed magnitude (kts) is shaded while the temperature (K) and geopotential height (m) anomalies and the 2-PVU isosurfaces are indicated by the black, gray, and green contours, respectively while the red lines at each analysis level indicate the size of the kinematic variable removal region. Once again, continuity between the respective kinematic and thermodynamic variables is preserved along the boundaries of the TC vortex removal region. Finally, Figure 3 provides a histogram illustrating the total number of smoothing operator applications
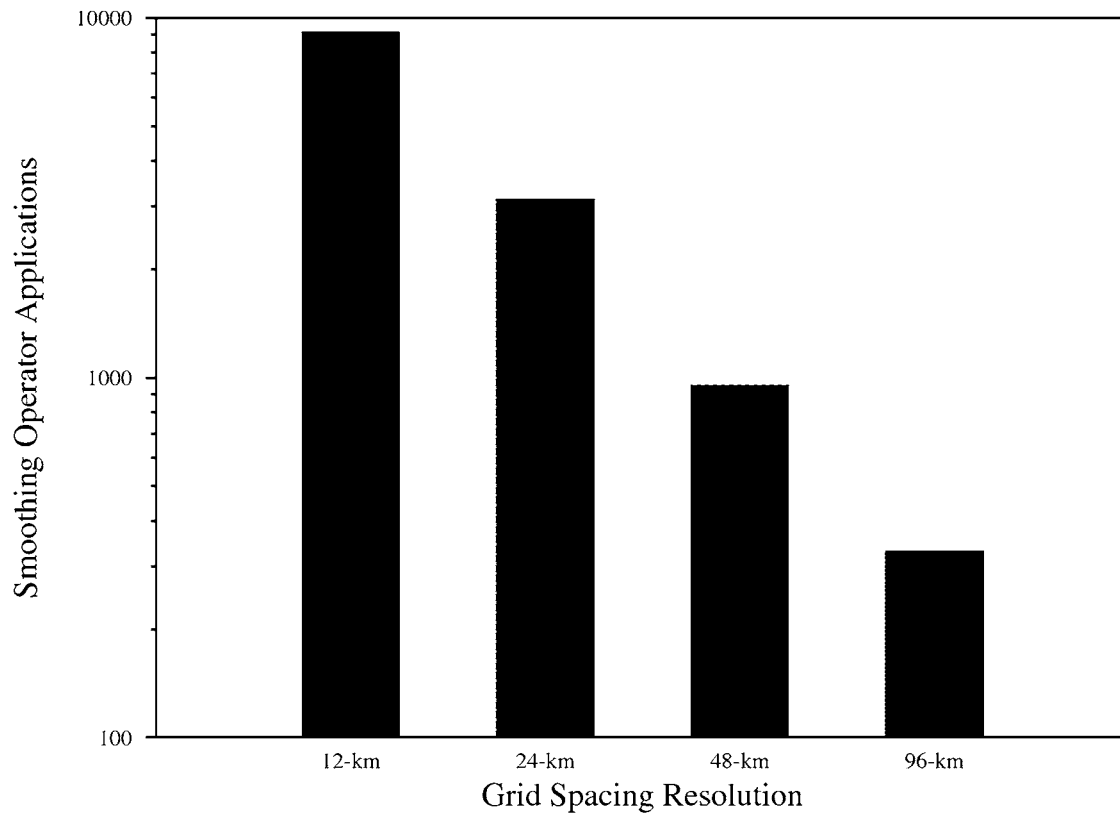
required to remove TC Gustav (2008) within the NCEP GFS sea-level pressure analysis as a function of different grid-spacing resolutions. This result indicates that, although the algorithm does not require tuning as a function of the grid spacing resolution, the number of smoothing operator applications required to converge to the respective $\Delta\sigma^2$ decreases by nearly an order of magnitude as the grid spacing resolution becomes increasingly coarse.

2.3. Initializing the Model Analysis After the TC Vortex Removal

The TC vortex removal procedure, described here does not employ physical constraints, thus imbalances within the respective *smoothed* analysis variables are inevitably induced. Therefore, the application of dynamical balancing and/or model initialization may be required. For this study, the
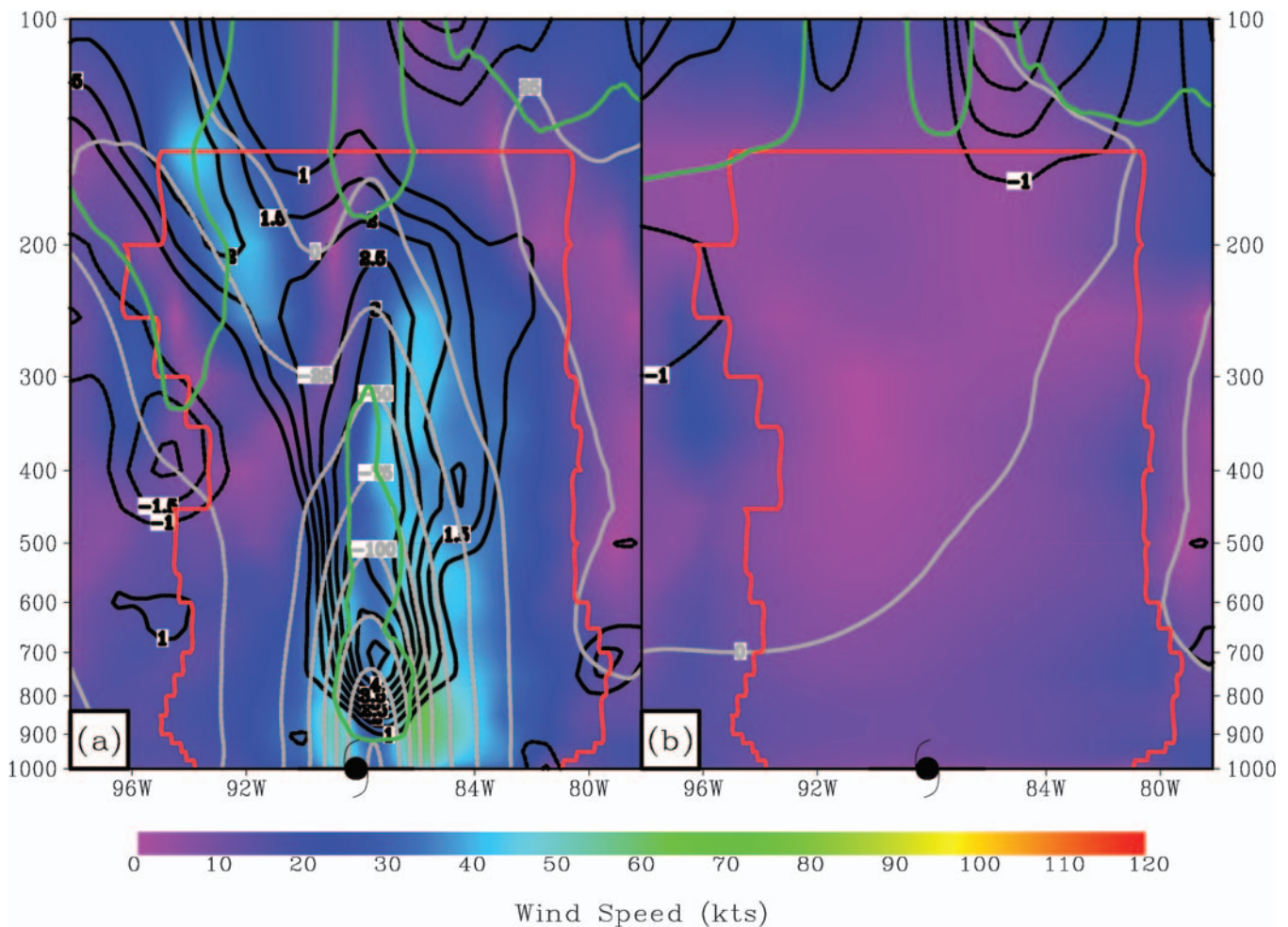
Figure 2. Vertical cross-sections for the kinematic and thermodynamic analysis variables, defined on a 6.0-km WRF-ARW model simulation grid, centered at the 0000 UTC 01 September NCEP GFS analysis position for TC Gustav (2008) (a) before and (b) after the application of the TC vortex removal algorithm. The shading is the wind-speed (kts), while the temperature and geopotential height anomalies are indicated by the black and gray contours, respectively. The anomaly fields for the temperature and geopotential are computed using a $\pm$ 10°areal mean centered at the analysis position (indicated by the cyclone symbol). The green and red lines are 2-PVU isosurfaces and the kinematic analysis variable removal region (as a function of analysis level), respectively.

Figure 3. Histograms illustrating the total number of smoothing operator applications required to remove TC Gustav (2008), as a function of the grid-spacing resolution, from the NCEP GFS sea-level pressure analysis interpolated to the WRF-ARW model simulation grid.

methodology discussed by *Stauffer and Seaman* [1990] and *Stauffer et al.* [1991] is used.

3. Algorithm Application

In this section, two experiments are compared. The first experiment (e.g., CNTRL) is a 120-hour simulation initialized from the 0000 UTC 15 September 2010 NCEP Global Data Assimilation System (GDAS) analysis. The NCEP GDAS is interpolated to a 9-km North-Atlantic Ocean (NATL) basin WRF-ARW model grid and contains TCs Karl (84.9W, 18.5N), Igor (53.5W, 18.9N), and Julia (30.5W, 16.3N). The second experiment (i.e., EXPT) is similar to CNTRL but each of the TC vortices within the WRF-ARW model domain have been removed using the

methodology provided in this study. Both forecast experiments are initialized from an analysis computed following 12-hour dynamic initialization. The physics parameterizations selected for these experiments are provided in Table 2.

Figure 4 illustrates the maximum 10-meter wind-speed magnitude (shaded) and minimum sea-level pressure (contour) swaths computed during 120-hour forecast. Figure 4a contains the results from CNTRL while Figure 4b depicts those from EXPT. An inter-comparison of Figures 4a and 4b, illustrates that the removal procedure has successfully suppressed the spin-up of TC-like features near the (initial) positions for the respective TCs. We note further that the positioning of larger-scale synoptic features (e.g., the subtropical ridge) is also similar. This suggests that the TC vortex removal procedure has successfully removed TCs

Table 2. Physics Parameterizations and the Respective Execution Frequencies (When Applicable) Used for the WRF-ARW Experiments.

Parameterized Physics	WRF-ARW Scheme
Microphysics	Lin et al.; called each model time-step
Longwave Radiation	Rapid Radiative Transfer Model (RRTM); called at 30-minute intervals during model integration
Shortwave Radiation	Dudhia; called at 30-minute intervals during model integration
Surface Layer Physics	Monin-Obukov (Janjic)
Surface Physics	Thermal diffusion
Boundary Layer Physics	Mellor-Yamada-Janjic Turbulent Kinetic Energy (TKE); called each model time-step
Cumulus Convection Physics	Betts-Miller-Janjic; called at 5-minute intervals during model integration
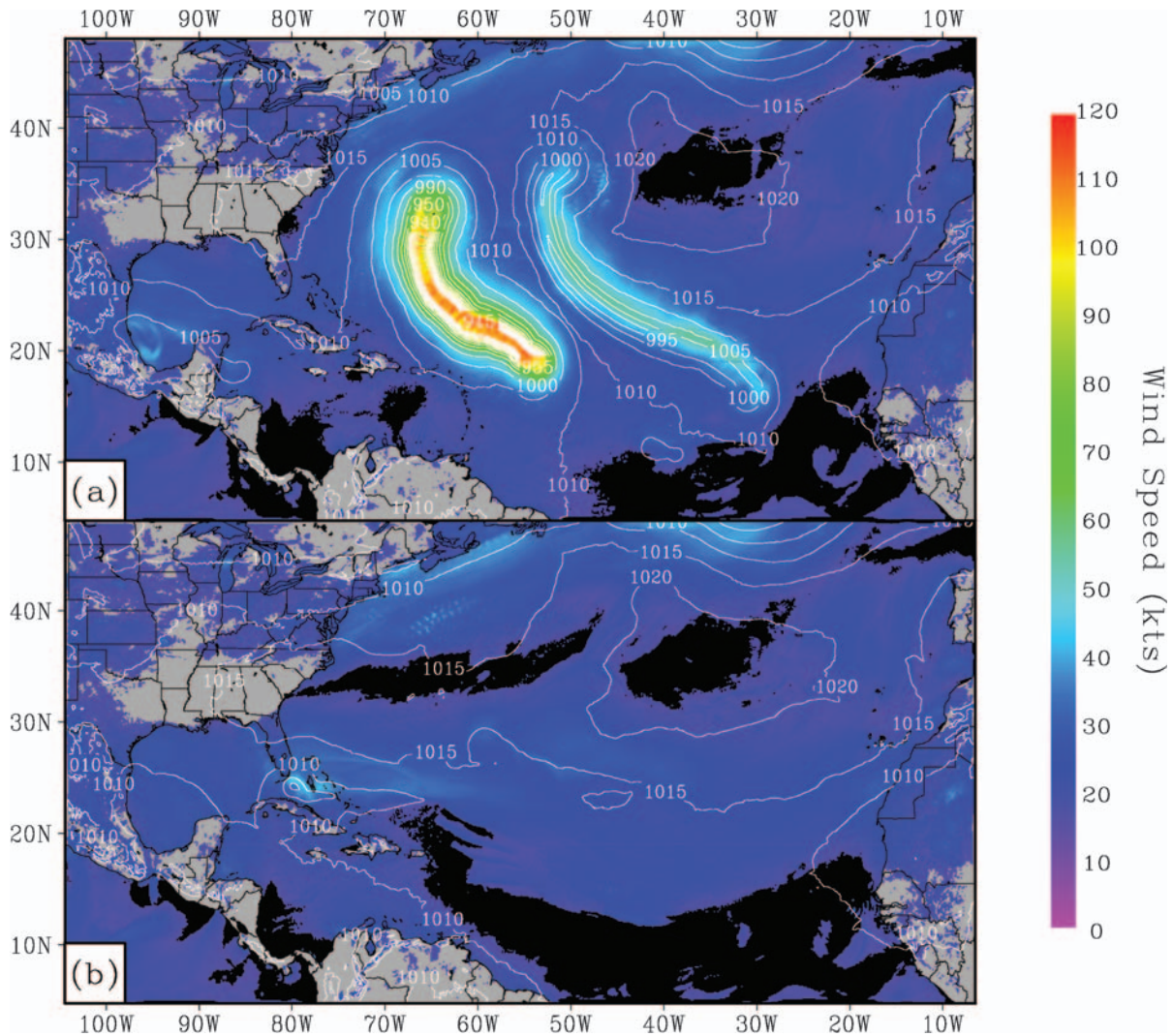
Figure 4. The maximum 10-meter wind-speed (kts; shaded) and minimum sea-level pressure (hPa; contour) swaths computed during the 120-hour forecast (a) CNTRL and (b) EXPT experiments, initialized at 0000 UTC 15 September 2010 from the NCEP GDAS analysis.

Igor, Julia, and Karl while simultaneously preserving the environments within the vicinity of the respective TCs.

An evaluation of the root-mean squared (RMS) differences between the CNTRL and EXPT analysis variables, which are computed as a function of the WRF-ARW forecast hour (not shown) suggest that the respective (simulated) atmospheres begin to evolve differently particularly beyond 48-hours. It seems as though this is a result of the TCs (or lack thereof) within the respective experiment initial conditions. This signal appears particularly in the upper-levels (e.g., 300- to 200-hPa) of the atmosphere while the lower atmosphere (specifically within the planetary boundary-layer) RMS differences for the humidity variable bifurcate beyond 72-hours. Finally, the RMS differences for P_{slp} also amplify as a function of time likely as a result of features that develop (or do not develop) in the wake of the simulated TCs. This specific application does not reveal

whether the increasing RMS differences are directly related to the presence of TCs within the model domain and/or a combination of the NWP model sensitivity to the respective CNTRL and EXPT initial conditions, the parameterization of the model physics, and/or the inherent non-linearity of the WRF-ARW prognostic variable tendency equations. Therefore the explicit determination for the TC impact upon the temporal and spatial scales of the atmosphere remains unfulfilled and is thus an active area of scientific research.

4. Conclusions and Discussion

In this study, a TC vortex removal algorithm is provided. The algorithm, in contrast to the existing alternative methods, is grid-spacing resolution independent and does not make assumptions regarding the size and structure of the TC. Rather, this scheme examines the attributes of the

kinematic and thermodynamic analysis variables and subsequently operates on the respective variables in order to provide prognostic NWP model variables that do not include the TC vortex. We accomplish this by prescribing separate kinematic and thermodynamic TC vortex removal regions that are tailored relative to the respective analysis TC. This sort of scheme may be useful, in particular for the statistical TC intensity prediction schemes (e.g., SHIPS/LGEM) that rely on larger scale predictors to produce their respective forecasts. Because we are limiting our modifications of the analysis variables to the spatial scales of the TC, the attributes of the environmental scales providing the predictor variables for the statistical methods remain largely unchanged beyond the confines of the TC.

The two experiments, CNTRL and EXPT, demonstrate that the algorithm is able to remove the (three) TC vortices within the WRF-ARW model domain while simultaneously preserving the synoptic scale atmosphere characteristics within the analysis. Although the RMS differences for the larger-scale features suggest that the model initial states (beyond the TC) are identical at the beginning of the WRF-ARW integration, the respective CNTRL and EXPT forecasts yield very different results. This was particularly the case for the kinematic variables within the upper-troposphere and the planetary boundary-layer thermodynamic variables. From Figure 4, we note the wind and P_{slp} swathes for EXPT suggest that a TC is nearing Miami, Florida. This similar feature is not evident in the results from CNTRL. These results both motivate and stimulate questions regarding the impacts for the TC(s) upon the larger-scale climate system. In particular the question whether the influence of the TC limited to the meso- and vortex-scales of the atmosphere or does the TC's influence cascade upscale to the larger global and climate time and space scales? Although these questions are beyond the scope of this particular study, they remain active areas of consideration and future research that can be investigated using the methodology provided in this study.

References

DeMaria, M. (1985), Tropical cyclone motion in a non-divergent barotropic model, *Mon. Weather Rev.*, **113**, 1199–1210, doi: 10.1175/1520-0493(1985)113<1199:TCMIAN>2.0.CO;2.

DeMaria, M. (2010), Tropical cyclone intensity change predictability estimates using a statistical-dynamical model, in *29th Conference on Hurricanes and Tropical Meteorology,* p. 9C.5, Am. Meteorol. Soc., Boston, Mass.

DeMaria, M., and J. Kaplan (1994), A Statistical Hurricane Intensity Prediction Scheme (SHIPS) for the Atlantic basin, *Weather Forecast.*, **9**, 209–220, doi: 10.1175/1520-0434(1994)009<0209:ASHIPS>2.0.CO;2.

DeMaria, M., M. Mainelli, L. K. Shay, J. A. Knaff, and J. Kaplan (2005), Further improvements to the Statistical Hurricane Intensity Prediction Scheme (SHIPS), *Weather Forecast.*, **20**, 531–543, doi: 10.1175/WAF862.1.

Elsberry, R. L., P. H. Dobos, and D. W. Titley (1993), Extraction of large-scale environmental flow components from the TCM-90 analyses: Implications for tropical cyclone motion studies, in *20th Conference on Hurricanes and Tropical Meteorology,* pp. 485–487, Am. Meteorol. Soc., Boston, Mass.

Fiorino, M., and R. L. Elsberry (1989), Some aspects of vortex structure related to tropical cyclone motion, *J. Atmos. Sci.*, **46**, 975–990.

Franklin, J. L., S. J. Lord, and F. D. Marks (1988), Dropwindsonde and radar observations of the eye of Hurricane Gloria (1985), *Mon. Weather Rev.*, **116**, 1237–1244, doi: 10.1175/1520-0493(1988)116<1237:DAROOT>2.0.CO;2.

Franklin, J. L., S. J. Lord, S. E. Feuer, and F. D. Marks (1993), The kinematic structure of Hurricane Gloria (1985) determined from nested analyses of dropwindsonde and Doppler radar data, *Mon. Weather Rev.*, **121**, 2433–2451, doi: 10.1175/1520-0493(1993)121<2433:TKSOHG>2.0.CO;2.

Gill, A. E. (1982), *Atmosphere–Ocean Dynamics*, 662 pp., Academic, New York.

Goerss, J. S. (2006), Prediction of tropical cyclone track forecast error for Hurricanes Katrina, Rita, and Wilma, in *27th Conference on Hurricanes and Tropical Meteorology,* p. 11A.1, Am. Meteorol. Soc., Boston, Mass.

Gray, W. M., and D. J. Shea (1973), The Hurricane's inner core region. II. Thermal stability and dynamic characteristics, *J. Atmos. Sci.*, **30**, 1565–1576, doi: 10.1175/1520-0469(1973)030<1565:THICRI>2.0.CO;2.

Hasler, A. F., and K. R. Morris (1986), Hurricane structure and wind fields from stereoscopic and infrared satellite observations and radar data, *J. Appl. Meteorol.*, **25**, 709–727, doi: 10.1175/1520-0450(1986)025<0709:HSAWFF>2.0.CO;2.

Hsiao, L.-F., C.-S Liou, T.-C Yeh, Y.-R Guo, D.-S Chen, K.-N. Huang, C.-T. Terng, and J.-H. Chen (2010), A vortex relocation scheme for tropical cyclone initialization in advanced research WRF, *Mon. Weather Rev.*, **138**, 3298–3315, doi: 10.1175/2010MWR3275.1.

Knaff, J. A., C. R. Sampson, and M. DeMaria (2005), An operational statistical typhoon intensity prediction scheme for the western North Pacific, *Weather Forecast.*, **20**, 688–699, doi: 10.1175/WAF863.1.

Kurihara, Y., M. A. Bender, and R. J. Ross (1993), An initialization scheme of hurricane models by vortex specification, *Mon. Weather Rev.*, **121**, 2030–2045, doi: 10.1175/1520-0493(1993)121<2030:AISOHM>2.0.CO;2.

Kurihara, Y., M. A. Bender, R. E. Tuleya, and R. J. Ross (1995), Improvements in the GFDL Hurricane Prediction System, *Mon. Weather Rev.*, **123**, 2791–2801, doi: 10.1175/1520-0493(1995)123<2791:IITGHP>2.0.CO;2.

La Seur, N. E., and H. F. Hawkins (1963), An analysis of Hurricane Cleo (1958) based on data from research reconnaissance aircraft, *Mon. Weather Rev.*, **91**, 694–709, doi: 10.1175/1520-0493(1963)091<0694:AAOHCB>2.3.CO;2.

Lord, S. J. (1991), A bogussing system for vortex circulations in the National Meteorological global forecast model, in *19th Conference on Hurricanes and Tropical Meteorology*, pp. 328–330, Am. Meteorol. Soc., Boston, Mass.

Marchok, T. P. (2002), How the NCEP tropical cyclone tracker works, in *25th Conference on Hurricanes and Tropical Meteorology*, pp. 21–22, Am. Meteorol. Soc., Boston, Mass.

Marks, F. D., and R. A. Houze (1987), Inner core structure of Hurricane Alicia from airborne Doppler radar observations, *J. Atmos. Sci.*, **44**, 1296–1317, doi: 10.1175/1520-0469(1987)044<1296:ICSOHA>2.0.CO;2.

Mathur, M. B. (1991), The National Meteorological Center's quasi-Lagrangian model for hurricane prediction, *Mon. Weather Rev.*, **119**, 1419–1447, doi: 10.1175/1520-0493(1991)119<1419:TNMCQL>2.0.CO;2.

Ritchie, E. A., and W. M. Frank (2007), Interactions between simulated tropical cyclones and an environment with a variable Coriolis parameter, *Mon. Weather Rev.*, **135**, 1889–1905, doi: 10.1175/MWR3359.1.

Sampson, C. R., J. L. Franklin, J. A. Knaff, and M. DeMaria (2008), Experiments with a simple tropical cyclone intensity consensus, *Weather Forecast.*, **23**, 304–312, doi: 10.1175/2007WAF2007028.1.

Shea, D. J., and W. M. Gray (1973), The Hurricane's inner core region. I. Symmetric and asymmetric structure, *J. Atmos. Sci.*, **30**, 1544–1564, doi: 10.1175/1520-0469(1973)030<1544:THICRI>2.0.CO;2.

Skamarock, W. C., J. B. Klemp, J. Dudhia, D. O. Gill, D. M. Barker, W. Wang, and J. GPowers (2005), A description of the Advanced Research WRF Version 2, *NCAR Tech. Note 468+STR*, Natl. Cent. for Atmos. Res., Boulder, Colo.

Stauffer, D. R., and N. LSeaman (1990), Use of four-dimensional data assimilation in a limited-area meso-scale model. Part I: Experiments with synoptic-scale data, *Mon. Weather Rev.*, **118**, 1250–1277, doi: 10.1175/1520-0493(1990)118<1250:UOFDDA>2.0.CO;2.

Stauffer, D. R., N. L. Seaman, and F. SBinkowski (1991), Use of four-dimensional data assimilation in a limited–area mesoscale model. Part II: Effects of data assimilation within the planetary boundary layer, *Mon. Weather Rev.*, **119**, 734–754, doi: 10.1175/1520-0493(1991)119<0734:UOFDDA>2.0.CO;2.

Velden, C. S., and L. MLeslie (1991), The basic relationship between tropical cyclone intensity and the depth of the environmental steering layer in the Australian region, *Weather Forecast.*, **6**, 244–253, doi: 10.1175/1520-0434(1991)006<0244:TBRBTC>2.0.CO;2.